

# A 114GHz Biosensor with Integrated Dielectrophoresis for Single Cell Characterization

Ali Ameri<sup>1</sup>, Luya Zhang<sup>1</sup>, Asmaysinh Gharia<sup>1</sup>, Mekhail Anwar<sup>2</sup>, Ali M. Niknejad<sup>1</sup>

<sup>1</sup>University of California, Berkeley, CA, <sup>2</sup>University of California, San Francisco, CA

## Abstract

A 114GHz permittivity biosensor for characterization of single biological cells is demonstrated. The sensor takes advantage of integrated dielectrophoresis for precise sample positioning resulting in higher sensitivity. The sensor detects a 0.73% change in the permittivity in a 1 KHz BW and identifies cells in their different stages of division as well as differentiating various cell lines.

## Introduction

The fundamental challenge in cancer therapy is identifying cells with aberrant cell division and specifically halting, or killing, those cells, while preserving surrounding healthy or normal cells. This requires active sensing, feedback and control at the signal cell level with real-time physician input, lending itself to an all-electronic approach demanding a mechanism of (1) identifying tumor cells, (2) classifying their cell division, and (3) ultimately inhibiting their growth is needed. Recently, the ability to inhibit cell division with electromagnetic fields was demonstrated in a clinical trial [1], showing a survival advance in a highly aggressive brain tumor, glioblastoma, but an all-electronic method of identifying and classifying cells remains unsolved.—mmWave sensing a promising technique to provide insight into differences between cell types and dynamic internal cellular changes as it bypasses the cell membrane and interacts directly with constituent biomolecules. mmWaves have been used to image the real-time growth of microorganisms [2] and identify cells in high-speed flow cytometer [3]. These platforms rely on sensing the perturbations in highly localized electric fields when interacting with the sample.

In this work, we significantly advance millimeter-wave cellular sensing by increasing sensing frequency, and enhancing sensitivity thorough precise positioning of samples on the sensing sites using integrated dielectrophoresis (DEP) [4]. We demonstrate both identification and *characterization of cell division state* in single cells with 114GHz permittivity sensor realized in a 28nm bulk CMOS process.

## Sensor Architecture

Fig. 1(a) shows the sensor core consisting of a sensing oscillator injection-locked to a reference oscillator. The sensing resonator is exposed to the sample, while the reference resonator is protected from the sample. A change in the dielectric constant of the sample on the sensing resonator introduces a phase shift ( $\phi$ ) at the output of the sensing oscillator. The oscillator signals are subsequently buffered and drive the quadrature hybrid input ports. The two outputs of the hybrid, which consist of the summation of the two oscillator signals in quadrature, are self-mixed in non-linear blocks to extract the desired phase signal,  $\phi$ .

Fig. 1(b). shows the circuit details of each block. The oscillator core ( $M_1$ - $M_2$ ,  $L_1$ ) directly drives the buffering stage ( $M_3$ - $M_4$ ,  $L_2$ ), while  $L_2$  is coupled to  $L_1$  with a coupling factor,  $k_1$ . Due to this coupling effect, two oscillation modes at  $\omega_0 = 1/\sqrt{L(1 \pm k)\bar{C}}$  are possible where the lower mode was chosen in this design [5]. This built-in buffering scheme in the oscillators achieves a small footprint allowing placement of the two oscillators close together for better matching and minimizing unwanted phase delays in the injection path.  $M_5$ - $M_6$  are the injection devices driven by the buffered output of the reference oscillator and tied to a fixed voltage for the sensing and the reference oscillators, respectively. The reference oscillator operates at 112 GHz with 4 GHz tuning range using varactors. The frequency offset between oscillators due to mismatches and different material loading is cancelled by tuning the control voltage of the sensing oscillator.

The buffered oscillator outputs are ac-coupled to another two-stage tuned buffer. These neutralized buffers are inductively coupled to achieve a large bandwidth and to suppress any common-mode signals originating from oscillator mismatches. The output of the buffers drives the two isolated input ports of the quadrature hybrid and the through and coupled ports provide the outputs. This results in the summation of two signals in quadrature, suitable for phase detection without offset. The quad hybrid, which is realized with lumped capacitors and inductors, is terminated and ac-coupled to the mixers. The mixer consists of two NMOS devices biased near threshold voltage to maximize the device nonlinearity, and performs self-mixing of its input. The tied drain of the two devices suppresses the fundamental tone and a resistive load is chosen to reduce the 1/f noise. The desired phase information at the output of the mixers is chopped and amplified by a VGA.

## Packaging

A microfluidic structure interfaces with the chip for continuous delivery of samples. Fig. 2 shows the package consisting of a ~80 $\mu$ m tall PDMS structure on the chip to form a 70 $\mu$ m wide channel and vertical holes as inlet and outlet. A stack of a glass slide and a second layer of PDMS branch out the inlet and outlet for external tubing. O<sub>2</sub> plasma treatments and mechanical pressure seal the layers.

## Material Sensing

Initial testing was performed by injection of various liquids into the channel. In Fig. 3(a) a clear change in the sensor output for each material is observed. The real part of the dielectric constants of DI water and air at 114GHz are 7.5 and 1, respectively, translating to a 15mV change in the sensor output for  $\Delta\epsilon=1$ . Based on the output noise PSD, shown in Fig. 3(b), and assuming a 1 KHz bandwidth for high-speed flow cytometry applications, the total output noise of the sensor is 0.11mVrms, meaning that a minimum 0.73% change in the sample permittivity is detectable (SNR=1).

For DEP functionality tests and visualizing cell division, cells expressing Green Fluorescent Protein (GFP) (enabling fluorescence microscopy), were suspended in a standard low-conductivity solution, allowing DEP. With DEP activated at 20 MHz, cells are captured and moved to the desired locations for optimal sensing, as shown in Fig. 4.

## Cell Sensing

The sensor's ability to differentiate various cell lines was demonstrated using HTC-116 (n=57), HeLa GFP (n=58) and SK-MEL-28 (n=62) cell lines. Cell measurements were taken with a VGA gain of 10 and a chopping frequency of 25MHz. Single cells were resuspended in a low-conductivity media (enabling pDEP), injected into the sensor channel for measurements. Fig. 5(a) shows a clear distinction between the measured signal from these cell lines which confirms the high sensitivity and selectivity of this sensor.

Furthermore, sensing the cell division for one of the cell lines was investigated. HeLa cells were cultured and synchronized in two different growth phases, Synthesis (S) phase and Mitosis (M) phase using Thymidine and Nocodazole [6]. 90 cells in M phase and 62 cells in S phase were measured with the sensor. As shown in Fig. 5(b) the sensor can detect the state of the cell without exogenous labels.

Chip micrograph and comparison table are shown in Fig. 6 and 7, respectively.

## References

[1] R. Stupp et al., *Jama* 314, no. 23, pp. 2535-2543, 2015. [2] T. Mitsunaka et al., *ISSCC*, pp. 478-479, Feb. 2016. [3] J.-C. Chien et al., *VLSI*, pp. 1-2, June 2014. [4] A. Ameri et al., Submitted to *Transducers* 2019. [5] B. Razavi, *JSSC*, vol. 46, no. 4 pp. 894-903, Apr. 2011. [6] H. Ma et al., *Methods Mol Biol*, vol. 761, pp. 151-161, 2011.

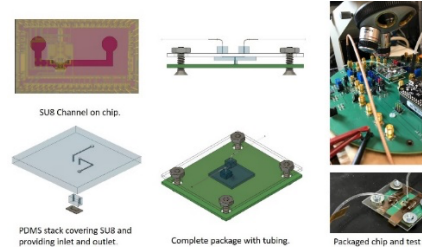
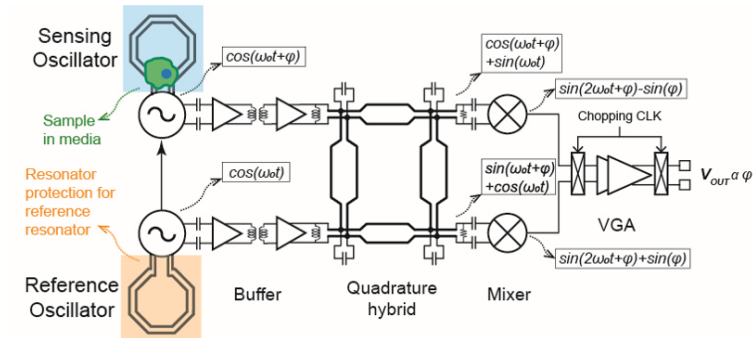


Fig. 2

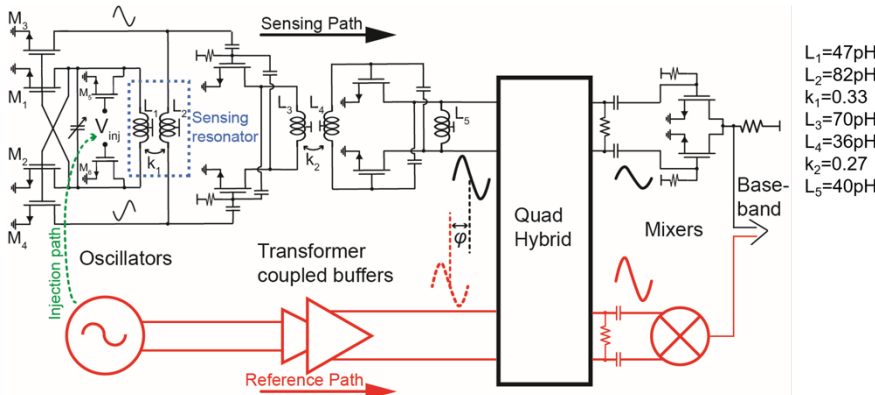


Fig. 1

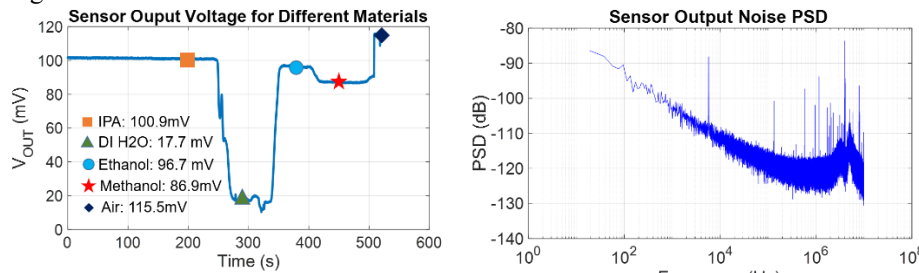


Fig. 3:

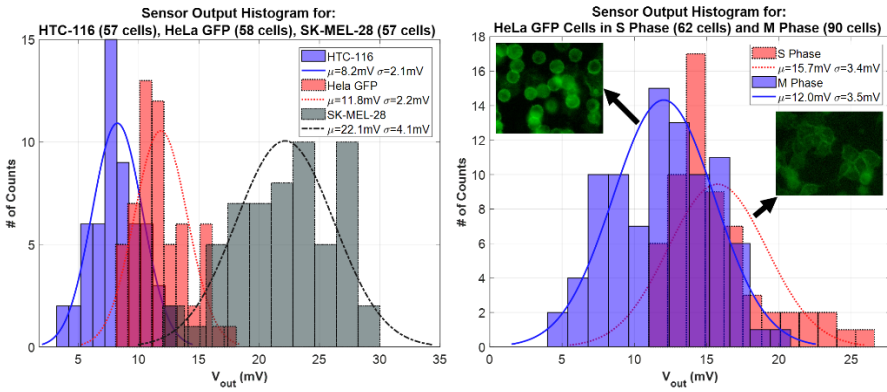


Fig. 5:

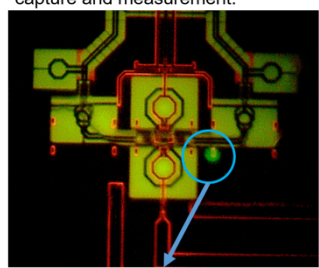
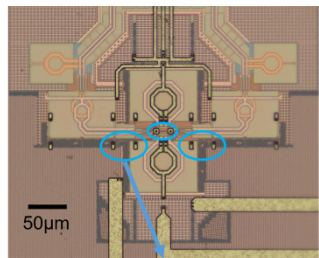


Fig. 4:

	Chien [3] VLSI 14	Mitsunaka [2] ISSCC 16	This work
Process	65nm	65nm	<b>28nm</b>
Label	None	None (Biological Water)	<b>None</b>
Frequency	6.5 / 11 / 17.5 / 30 GHz	60 / 120 GHz	<b>114GHz</b>
Active area	$0.21\text{mm}^2$ (6.5GHz)	$0.008\text{mm}^2$ (60GHz) $0.014\text{mm}^2$ (120GHz)	<b><math>0.24\text{mm}^2</math></b>
Sample Manipulation	Flow	None	<b>DEP and flow</b>
Power consumption	65mW	47mW	<b>47mW</b>

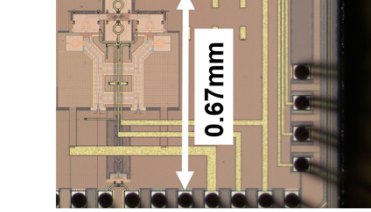


Fig. 6:

Fig. 7: